Comparative Study of Permanent Magnet Synchronous Machine vs Salient Pole Synchronous Machine in High Temperature Application

Romain Cousseau, Raphael Romary, François Balavoine, Miftah Irhoumah, Remus Pusca

Comparative Study of Permanent Magnet Synchronous Machine vs Salient Pole Synchronous Machine in High Temperature Application

Romain COUSSEAU, Raphaël ROMARY, François BALAVOINE, Miftah IRHOUMAH, Remus PUSCA
Univ. Artois, UR 4025, Laboratoire Systèmes Electrotechnique et Environnement (LSEE)
F-62400 Béthune, France
romain.cousseau@univ-artois.fr

***Abstract*—This paper presents the sizing and the comparison of two synchronous machines. The purpose is to design a high temperature dedicated machine with the same performance as a permanent magnet machine. A salient pole wound rotor is chosen with anodized aluminum tape as windings.**

Keywords— Motor sizing, high temperature, permanent magnet, anodized aluminum tape, thermal study.

I. INTRODUCTION

In a large variety of fields, electrical machines are more and more preferred to traditional actuators (pneumatics or hydraulics) [1]. Indeed, thanks to their compactness and efficiency, machines like PMSM (Permanent Magnet Synchronous Machine) are very attractive [2][3]. However, because of the use of permanent magnets, this kind of machine is not very suitable for harsh environment where temperature can be very high [4]. The aim of this paper is to present the sizing of two machine topologies of 40kW for 4500 rpm with similar size and performances. The first one is made with a permanent magnet rotor whereas the other one is made with a salient pole wound rotor to operate at high temperature. The second machine uses anodized aluminum tape [5][6] as windings because classical winding isolations are not appropriate at high temperature. The stator windings use the same conductor to hold the high temperature

The paper is organized as follows: Section II presents the sizing of a three-phase 12/10 (12 slots, 10 poles) synchronous machine with concentrated winding. Section III gives comparisons between the two machines through finite element simulations. Sections IV presents a complete thermal study for both machines. Section V brings explanation about the wound rotor construction. Section VI gives conclusions and highlights works that will be made for the future machine that is currently being build.

II. SIZING AND DESIGN OF THE MACHINES

A. Main dimensions

First, it is necessary to find the main dimensions of the machine as a preliminary sizing process. The purpose is not to optimize the compacity of the machine but to get an easily achievable electrical motor.

To achieve that, the sizing formula in (1) is used. This is a simplified version of the sizing equation given in [7].

$$D_a{}^2 L_a = \frac{2C}{A\hat{B}\frac{K_1^s \pi}{\sqrt{2}}} \quad (1)$$

With D_a: the inner diameter of the stator, L_a: the active length, C: the rated torque, A: the current linear density, B: the peak airgap flux density and $K_1{}^s$: the winding factor.

The winding factor depends on the chosen topology such as the number of phases, slots and poles as explained in [8]. Considering (1), parameters are chosen as well as the active length to obtain a coherent stator diameter. The purpose is to obtain a mean torque of 100 Nm in a 0-4500rpm speed range for two machines: the first one is a reference machine with a permanent magnet rotor. The second machine has the same dimension than the reference one but with a wound rotor designed to provide the same magnetic effect than the permanent magnet rotor. In order to reach the same magnetic performance than the initial machine, the wound rotor machine used anodized aluminum tape able to operate at high temperature (more than 350°C). To simplify, both machines have the same stator, also made with anodized aluminum tape. Parameters are summed up in Table I.

TABLE I. DESIGN PARAMETERS

Torque C	100 N.m
Current linear density A	27000 A/m
Peak airgap flux density B	1.5 T
Winding factor $K_1{}^s$	0.933
Active length L_a	150 mm

This leads to an inner stator diameter of 126 mm.

Magnets have been taken the thickest of possible in order to be less sensitive to the temperature and to bring the highest flux density in the airgap, considering an interior magnet structure with flux concentration effect. Teeth wide has been determined to be minimum without being saturated.

Finally, the external diameter is 206 mm.

B. Winding determination

The method presented in [8] is used to determine the optimum winding sequence of the concentrated winding machine. The chosen structure of the machine is three-phase

This work has been achieved within the framework of CE2I project (Convertisseur d'Energie Intégré Intelligent). CE2I is co-financed by European Union with the financial support of European Regional Development Fund (ERDF), French State and the French Region of Hauts-de-France.

12/10 (12 stator slots, 10 poles) with double layer concentrated winding. At first, the SPP (number of slots per poles and per phase) needs to be determined (2).

$$SPP = 12/(3*10) = 2/5 \quad (2)$$

The purpose is to compare a sequence of "zeros" and "ones" to a reference sequence. According to the method, our comparative sequence will have 2 "ones" and 3 (5-2) "zeros" and will be "01010". The sequence is shown in Fig. 1 and the corresponding winding factor is 0.933.

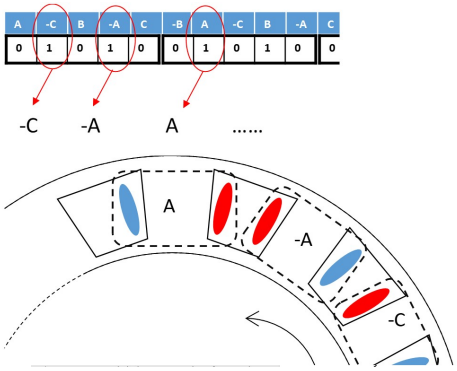

Fig. 1. Determination of the optimal winding sequence

C. *Results of the sizing*

Once sizing and winding have been determined, it is possible to draw both machines.

Fig. 2 and 3 show the two machine configurations having similar dimensions. For the wound rotor machine, saliencies have been designed to let enough space to place rotor windings. Based on these geometries, finite element simulations with Altair Flux 2D software will be performed in the next section.

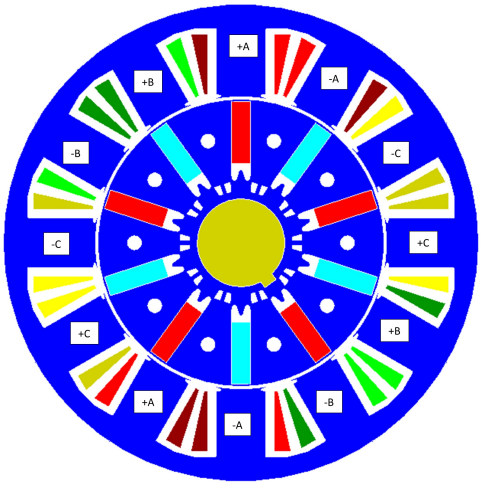

Fig. 2. Permanent magnet configuration

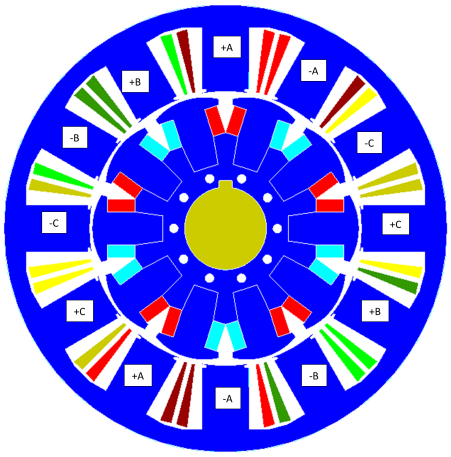

Fig. 3. Salient pole wound rotor configuration

III. Comparison of the Two Machines with Finite Element Simulation

A. *Performance comparison using torque and airgap flux density*

Performances of the two machines are compared through finite element simulations for the expected rated point (4500 rpm – 100Nm)

In a first step, the rotor direct current of the salient pole machine has been determined to achieve roughly the same airgap flux density than permanent magnet rotor, as shown in Fig. 4. Moreover, stator number of turns and stator current are similar for both machines. Stator number of turns are limited by the induced voltage that cannot exceed the DC bus voltage at maximum speed. The machine is powered with sine current and with flux-oriented control. Winding characteristics are summarized below.

- Stator windings: 10 coils per tooth (anodized aluminum tape of 0.4*24 mm)
- Stator current I_s: 80A peak (56.6A RMS - 6A/mm² current density)
- Rotor windings: 40 coils per pole (anodized aluminum tape of 0.15*12 mm)
- Rotor current I_r: 30A direct current (16A/mm² current density)

Fig. 5 presents the spectrum of the normal flux density in the airgap. As expected, the 5th harmonic is the principal because of the 5 pairs of poles. It is slightly higher for the permanent magnet machine but not significatively. However, some other harmonics like the 15th are higher.

Fig. 6 gives the torque of both machines at rated stator and rotor currents. It can be observed that the target torque was 100Nm but in both cases, simulated torques are weaker. This can be accounted for by assumptions used in the sizing formula. For example, the airgap flux density taken at 1.5T in (1) has roughly this value in the simulation for the peak value in Fig.4, but the fifth harmonic in Fig.5 falls to 0.85T.

Because of the magnet configuration, the PMSM is a flux concentration machine, that leads to a slightly higher induction in stator teeth (around 1.3 T vs 1.2 T for the wound

rotor machine). This can justify that the mean torques are not the same for both machines. Additionally, an interesting point is that the 12th harmonic (which corresponds to the number of slots) is the main one for the PMSM torque ripple whereas it is the 6th for the other rotor.

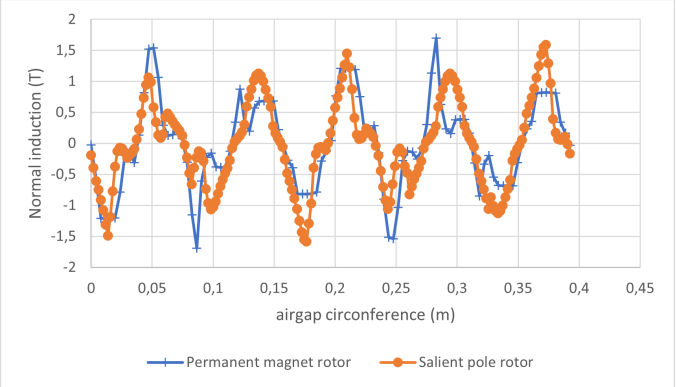

Fig. 4. Normal flux density comparison along an airgap lap

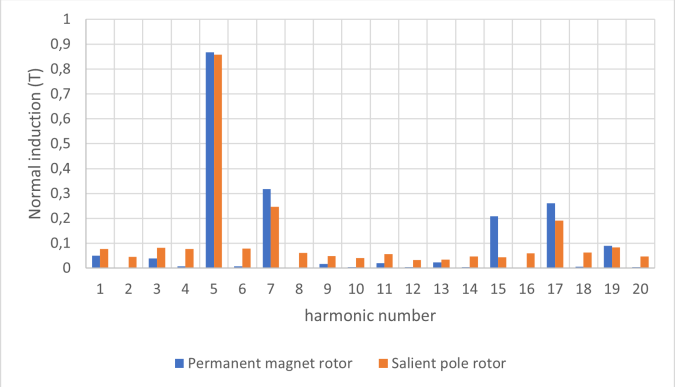

Fig. 5. Normal flux density spectrum comparison along an airgap lap

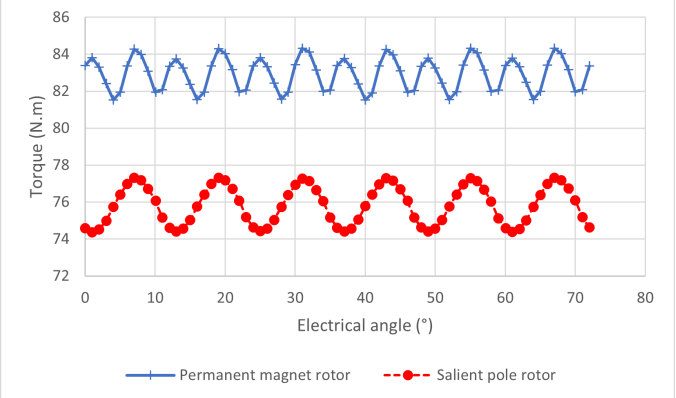

Fig. 6. Torque comparison at the rated operating conditions

B. *Flux lines comparison*

Fig. 7 and 8 present the mapping of flux lines for both machines. As it can be seen, the direction of the lines differs for the two rotors. They follow the pole in the radial way for the salient wound rotor whereas in the permanent magnet rotor they are oriented in orthoradial way. This is due to the magnetization direction that enable to have a flux concentration machine. Therefore, only a part of the magnet flux crosses the airgap. The other part flows towards the shaft, and this part can be reduced using a special shape at the level of the magnet inner part as shown in fig. 7.

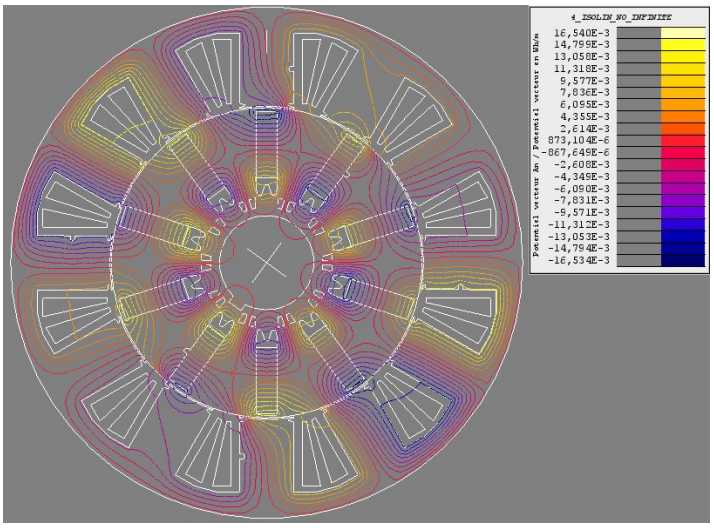

Fig. 7. Flux lines for the permanent magnet rotor machine

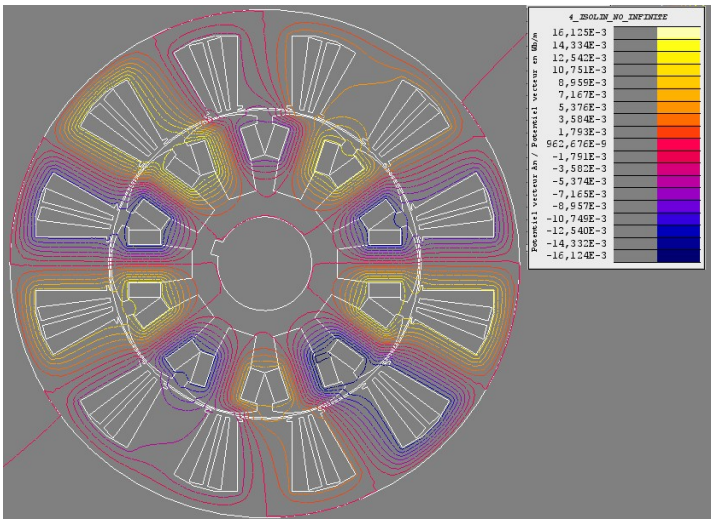

Fig. 8. Flux lines for the salient wound rotor machine

IV. THERMAL STUDY

A. *Power losses*

Losses have been obtained with Flux2D software and are summed up in Table II. These values correspond to the rated point (4500 rpm and rated current as described in section III).

TABLE II. LOSSES REPARTITION FOR BOTH MACHINES

Losses (W)	***Permanent magnet machine***	***Wound rotor machine***
Stator Joule	356	356
Rotor Joule	None	1827
Magnet	91	None
Stator iron	465	420
Rotor iron	76	48

Rotor Joule losses for the wound rotor seem to be quite important. This is due to the rotor direct current of 30A which is injected in a thin aluminum tape. Thus, the rotor electric resistance is relatively high (around 2Ω) what leads to high Joule losses. Comparatively, the stator current is higher (around 56A RMS), but the tape is wider and shorter so with a small electric resistance.

B. Geometry for the thermal study using Motor-Cad software

The machines that have been designed using Flux2D software for the finite element study have been rebuilt in the Motor-Cad software. Dimensions have been respected. The principal difference is the addition of a cooling part around the stator. This is a water jacket housing in a spiral. The characteristics of this cooling part are set to default in the software. An improvement of the cooling system could be made in further works.

C. Thermal results

From the losses in the different parts of the machines, a thermal study has been performed using Motor-Cad software. The ambient temperature is set to 20°C. Fig. 9, 10, 11 and 12 present temperatures at different critical points for both machines in axial and radial view.

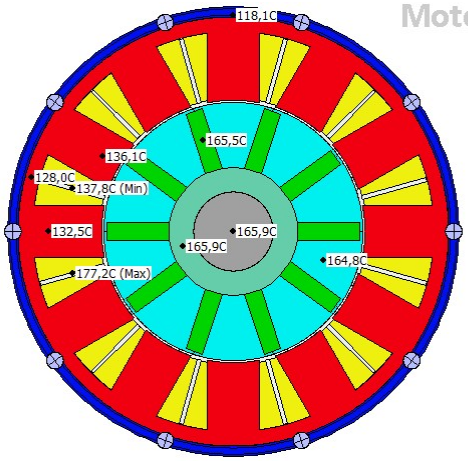

Fig. 9. Temperatures of the permanent magnet machine in radial view

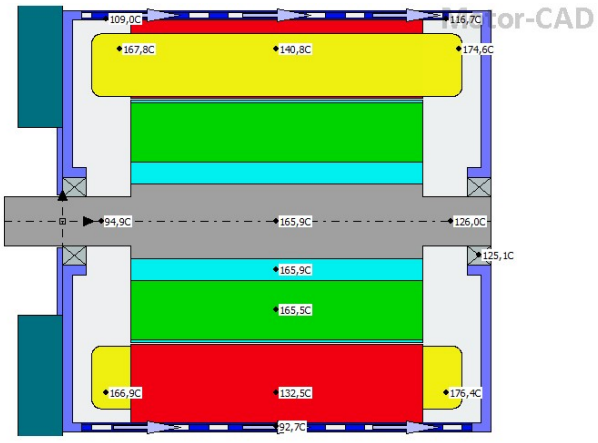

Fig. 10. Temperatures of the permanent magnet machine in axial view

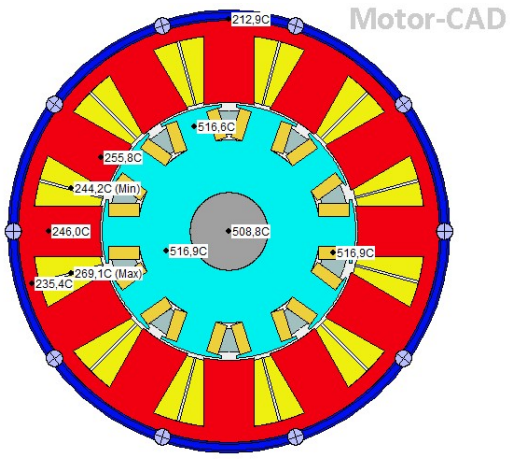

Fig. 11. Temperatures of the wound rotor machine in radial view

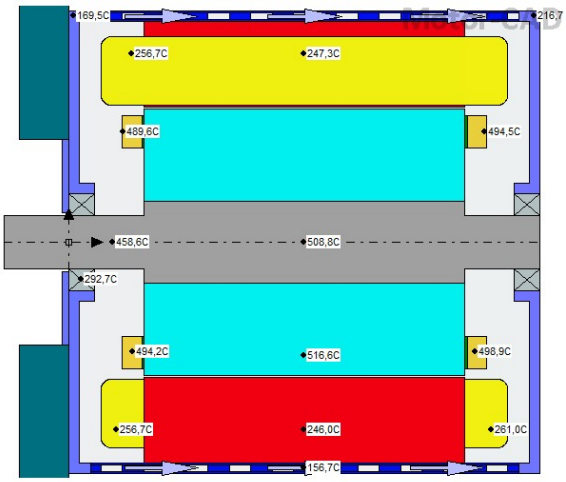

Fig. 12. Temperatures of the wound rotor machine in axial view

Presented results are given for steady state. This explains that temperatures can be rather high at specific critical points.

First, temperatures reached in the permanent magnet machine are quite usual as it can be found in other studies [9]. This leads to be optimistic about the quality of the simulations, both for losses determination and the thermal study. Moreover, the maximal temperature in magnets is less than 170°C. This is clearly in the range of the selected magnets which are Samarium Cobalt-based. This kind of magnet can usually withstand up to 300°C [10].

Considering pure aluminum, the welding temperature is around 660°C. In the worst case, which is the wound rotor machine, the highest temperature reached is less than 520°C thanks to the cooling. It should be noticed that to simplify the simulation, the evolution of the electric resistivity of the aluminum with temperature has not been considered. It means that at 400 or 500°C the electric resistance of the tape would be higher, leading to even more losses, and higher temperatures. However, this machine has been designed to obtain the same performances with a wound rotor than with a permanent magnet rotor at least for short time.

Another point to be considered is the bearings temperature. Classical bearings are not suitable to withstand such temperature (almost 300°C) [11]. So, in further works, a

full study should be made to design bearings with innovative materials that could hold these temperatures. A specific rotor cooling system could also be implemented.

D. Study in transient

Now that steady state has been studied, it can be interesting to see the evolution of some temperatures for a short period. This time, the ambient temperature starts from 40°C. Fig 13 and 14 presents transient evolution of the temperature at different points on both machines for one minute.

First, concerning the permanent magnet rotor machine, only the stator winding starts to heat but slowly (+6°C). This can be accounted for by stator joule losses that are quite low thanks to a small electric resistance and because the cooling device is close to these windings.

The same temperature rise is observed to the stator winding of the wound rotor machine. Indeed, the losses of the rotor do not have enough time to heat all the machine. However, the temperature in rotor windings rises quickly. It reaches 140°C (starting at 40°C) in less than one minute. The interesting point is that even if the shaft heats up also significantly, bearings are still relatively cold. This is reassuring concerning the experimental machine that is being built and it can be considered that tests could be executed for several minutes at rated operating conditions.

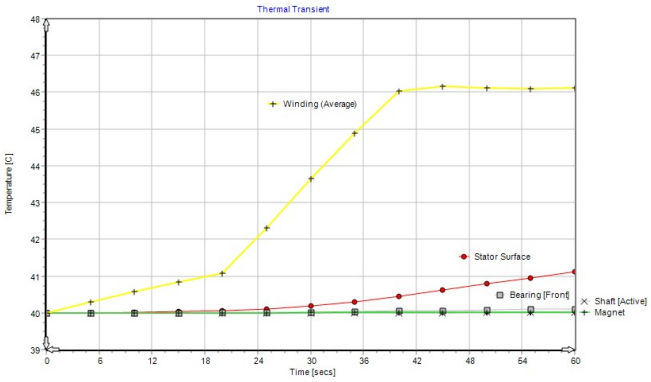

Fig. 13. Transient temperatures of characteristic points for the permanent magnet rotor machine

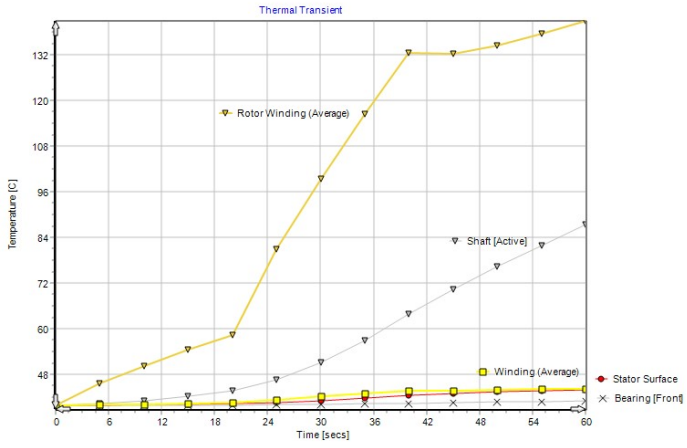

Fig. 14. Transient temperatures of characteristic points for the wound rotor machine

E. Thermal improvement in steady state

It has been shown previously that steady state temperatures for the wound rotor machine are quite high and would be even higher by considering the electric resistance increase. This could cause insulation deterioration or even critical failure in rotor windings.

To prevent any risk, a simple way to limit the heating is to decrease rotor direct current. In this case, airgap flux density will be lower than in the permanent magnet rotor machine. So, stator current needs to be increased to compensate and to obtain the same torque. By coupling losses and thermal analysis with a simple mathematical consideration, a new configuration is obtained. Table III sums up the results and compares values for the critical points.

As it can be observed, decreasing the rotor direct current by only 5 A leads to more than a 100°C reduction in windings rotor. An interesting fact is that even if stator current has been increased to get the same torque, stator temperatures are also lower. This means that for the wound rotor machine, heating is largely due to rotor losses. Moreover, the cooling water jacket is close to the stator so, it is easier to evacuate the heat in this area.

TABLE III. COMPARISON OF THE TWO CONFIGURATIONS FOR THE WOUND ROTOR MACHINE

	Old configuration	***New configuration***
Current rotor I_r	30 A	25 A
Rotor Joule losses	1800 W	1264 W
Current stator (peak) I_s	80 A	92 A
Stator Joule losses	356 W	471 W
Torque (average)	76 Nm	77 Nm
Rotor highest temperature (winding)	517°C	406°C
Stator highest temperature (winding)	269°C	237°C

V. ROTOR WINDING REALIZATION

As previously explained, the winding is quite unusual because it is made of anodized aluminum tape. So, it is interesting to present technical solutions that have been chosen to make the windings, especially concerning the rotor.

First, rotor windings are coiled up around a plot corresponding to a rotor pole. Then, each plot will be screwed to the main piece of the rotor. Fig. 15 shows one plot with the anodized aluminum tape around. In the final version, each winding will be protected with fiberglass paper and filled up with a high temperature resin to ensure good rigidity and isolation. Because this kind of tape is relatively brittle and the rotor will turn up to 4500 rpm, a solution has been developed to ensure a good stability and to connect the ten poles together. This is achieved with a connection disk attached to the rotor. One part of the tape goes through the disk and is screwed to the part of the tape from the direct next pole. Concerning the two parts of tape in contact on the disk, the anodized isolated surface has been removed. The disk is made in PEEK which is a polymer with good structural characteristics and a high welding point (343°C).

Fig. 16 presents the connectivity principle on the disk. The same idea has been developed for stator connectivity.

Fig. 15. Example of winding around a pole rotor

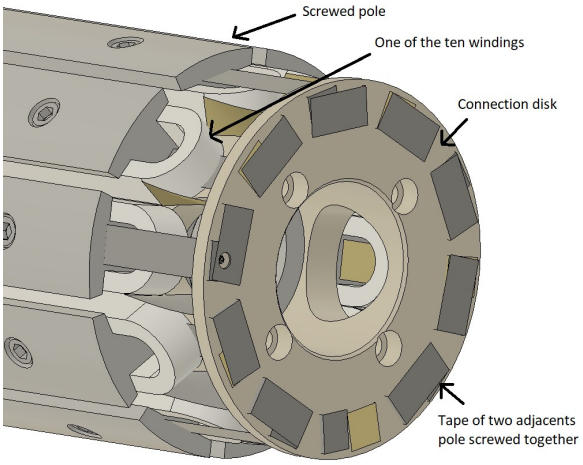

Fig. 16. Connection disk for the rotor winding

VI. Conclusions and Perspectives

This paper proposes a design of synchronous machines with the purpose to obtain the performances of PMSM with a salient pole wound rotor machine that can operate at higher temperature.

First, a sizing method has been presented and main dimensions have been given. Also, the way to find the ideal winding sequence has been presented.

Then, finite element simulations have been carried out with Flux2D software to compare the performances of the two machines with the same stator configuration. It appears that the obtained torque is quite similar with a small advantage for the permanent magnet rotor machine. This has been explained previously.

Thanks to these simulations, Joule losses and iron losses have been determined and used in the Motor-Cad software to evaluate temperatures both in steady state and in transient. It appears that the permanent magnet rotor machine ends with totally acceptable temperatures especially concerning magnets. However, temperatures reached in the wound rotor machine are relatively high and could deteriorate the machine especially the insulation in rotor windings. So, another configuration has been presented by decreasing rotor direct current and increasing stator current. Results show a better heat repartition and more than a 100°C decrease for critical parts (rotor windings) while performances are not altered. Problems concerning some exterior parts such as classical bearings that cannot handle such temperature have been evocated.

From a technical point of view, the way to create winding with anodized aluminum tape has been shown.

Finally, design and simulated results have been conducted successfully with promising results to get a high temperature machine with great performances while avoiding magnets and classical winding that are not suitable with such temperatures.

Future works will consist of testing these machines which are currently being built in real conditions. Moreover, a study about the efficiency of both machines needs to be carried out and the environmental impact of these two technologies needs to be evaluated.

References

[1] M. Lefik, K. Komeza, E. Napieralska Juszczak, D. Roger, P. Napieralski, N. Takorabet and H. Elmadah, “High temperature machines: topologies and premilinary design,” De Gruyter, Open Phys. 2019, 17: pp. 657-669.

[2] Z. Q. Zhu and D. Howe, “Electrical machines and drives for electric, hybrid, and fuel cell vehicles,” Proceedings of the IEEE, 2007, vol. 95, no. 4, pp. 746–765.

[3] M. N. Uddin, T. S. Radwan, and M. A. Rahman, “Performance of interior permanent magnet motor drive over wide speed range,” IEEE International Electric Machines and Drives Conference, IEMDC 1999 - Proceedings, 1999, vol. 17, no. 1, pp. 31–33.

[4] T. Huber, W. Peters and J. Böcker, “Monitoring critical temperatures in permanent magnet synchronous motors using low-order thermal models,” IPEC-Hiroshima 2014 - ECCE Asia, Hiroshima, Japan, 2014, pp. 1508-1515.

[5] S. Babicz, S. Ait-Amar Djennad, and G. Velu, “Preliminary study of using anodized aluminum strip for electrical motor windings,” IEEE Conference on Electrical Insulation and Dielectric Phenomena (CEIDP). IEEE, 2014.

[6] S. Babicz, S. Ait-Amar, and G. Velu, “Dielectric characteristics of an anodized aluminum strip,” IEEE Transactions on Dielectrics and Electrical Insulation 23.5, 2016, pp. 2970-2977.

[7] B. Cassoret, J. P. Lecointe and J. F. Brudny, “Influence of the Pole Number on the Magnetic Noise of Electrical AC Machines,” Progress In Electromagnetics Research B. 2011, pp. 83-97.

[8] F. Libert and J. Soulard, “Investigation on pole-slot combinations for permanent-magnet machines with concentrated windings,” International Conference on Electrical Machines, January 2004, pp. 5–8.

[9] G. Guedia Guemo, P. Chantrenne and J. Jac, “Application of Classic and T Lumped Parameter Thermal Models for Permanent Magnet Synchronous Machines,” International Electric Machines & Drives Conference, Chicago USA, 2013, pp. 809-815.

[10] J. F. Liu and M. H. Walmer, “Thermal stability and performance data for SmCo 2:17 high-temperature magnets on PPM focusing structures,” IEEE Transactions on Electron Devices 52, 2005, pp. 899-902

[11] J.A. Henao-Sepulveda, M. Toledo-Quiñones and Y. Jia, “Contactless Monitoring of Ball Bearing Temperature,” IMTC 2005 – Instrumentation and Measurement Technology Conference, Ottawa, Canada, 17-19 May, 2005, pp. 1571-1573

[12] S. Xiaoyong, C. Liangcheng, M. Honglin, G. Peng, B. Zhanwei and L. Cheng, “Experimental Analysis of High Temperature PEEK Materials on 3D Printing Test,” 9th International Conference on Measuring Technology and Mechatronics Automation (ICMTMA), Changsha China, 2017, pp. 13-16